

# The Post-Translational Modification in Cytochrome *c* Oxidase Is Required To Establish a Functional Environment of the Catalytic Site<sup>†</sup>

Tapan Kanti Das,<sup>‡</sup> Catherine Pecoraro,<sup>§</sup> Farol L. Tomson,<sup>§</sup> Robert B. Gennis,<sup>§</sup> and Denis L. Rousseau<sup>\*,‡</sup>

Department of Physiology and Biophysics, Albert Einstein College of Medicine, 1300 Morris Park Avenue, Bronx, New York 10461, and School of Chemical Sciences, University of Illinois, 600 South Mathews Street, Urbana, Illinois 61801

Received June 25, 1998; Revised Manuscript Received August 24, 1998

**ABSTRACT:** Mutation of tyrosine-288 to a phenylalanine in cytochrome *c* oxidase from *Rhodobacter sphaeroides* drastically alters its properties. Tyr-288 lies in the Cu<sub>B</sub>–cytochrome *a*<sub>3</sub> binuclear catalytic site and forms a hydrogen bond with the hydroxy group on the farnesyl side chain of the heme. In addition, through a post-translational modification, Y288 is covalently linked to one of the histidine ligands that is coordinated to Cu<sub>B</sub>. In the Y288F mutant enzyme, the “as-isolated” preparation is a mixture of reduced cytochrome *a* and oxidized cytochrome *a*<sub>3</sub>. The cytochrome *a*<sub>3</sub> heme, which is largely six-coordinate low-spin in both oxidation states of the mutant, cannot be reduced by cytochrome *c*, but only by dithionite, possibly due to a large decrease in its reduction potential. It is postulated that the Y288F mutation prevents the post-translational modification from occurring. As a consequence, the catalytic site becomes disrupted. Thus, one role of the post-translational modification is to stabilize the functional catalytic site by maintaining the correct ligands on Cu<sub>B</sub>, thereby preventing nonfunctional ligands from coordinating to the heme.

Cytochrome *c* oxidase (CcO) is the terminal respiratory enzyme that catalyzes the reduction of dioxygen to water using electrons supplied by its physiological substrate, ferrocytochrome *c*. The redox processes are coupled to proton translocation in which one proton for each electron is translocated across the inner mitochondrial membrane in the eukaryotic enzyme (1–17). In addition, an additional (scalar) proton, per each electron, is taken up from the matrix side of the membrane in the formation of water. The oxygen reaction occurs at a binuclear site composed of Cu<sub>B</sub> and the heme group of cytochrome *a*<sub>3</sub>. The reduced heme in cytochrome *a*<sub>3</sub>, a five-coordinate high-spin complex with a histidine axial ligand, binds oxygen rapidly to initiate the enzymatic reaction. Two additional redox centers, cytochrome *a* and another binuclear center referred to as Cu<sub>A</sub>, are involved in the electron transfer pathway from ferrocytochrome *c* to the cytochrome *a*<sub>3</sub>–Cu<sub>B</sub> catalytic site.

Crystal structures of several forms of cytochrome *c* oxidase have been reported and reveal some very interesting features (see Figure 1). The distance (*d*) between the iron atom of cytochrome *a*<sub>3</sub> and Cu<sub>B</sub> is very small and is apparently variable. In the structure of the resting bovine enzyme reported by Tsukihara et al. (2), the distance was 4.5 Å, whereas in the structure of the azide-inhibited four-subunit *Paracoccus denitrificans* enzyme reported by Iwata et al.

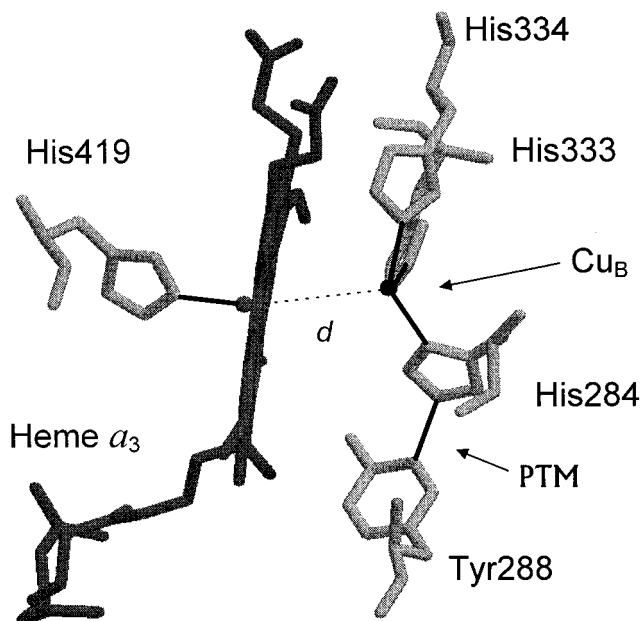


**FIGURE 1:** Binuclear center of the two-subunit cytochrome *c* oxidase from *P. denitrificans* (4) in the oxidized state. The coordinates (1ar1) were taken from the Brookhaven Protein Data Bank. The residue numbering of *R. sphaeroides* is adopted here. Shown in the structure are heme *a*<sub>3</sub>, coordinated to His419, and Cu<sub>B</sub>, bound to three histidines, His-333, His-334, and His-284. The distance (*d*) between the iron atom of cytochrome *a*<sub>3</sub> and Cu<sub>B</sub> is designated by the dotted line. The Tyr-288–His-284 cross-linking due to post-translational modification (PTM) is also shown. It is postulated that in the Y288F mutant the PTM is absent.

(1), the distance was 5.2 Å. For the structure of the oxidized complex of the two-subunit *P. denitrificans* oxidase, Ostermeier et al. (4) report a distance of 4.5 Å, similar to that in

<sup>†</sup> This work was supported by NIH Grants GM54806 and GM54812 to D.L.R. and HL16101 to R.B.G.

<sup>\*</sup> To whom correspondence should be addressed: Department of Physiology and Biophysics, Albert Einstein College of Medicine, 1300 Morris Park Ave., Bronx, NY 10461. Telephone: (718) 430-4264. Fax: (718) 430-4230. E-mail: rousseau@aecom.yu.edu.

<sup>‡</sup> Albert Einstein College of Medicine.

<sup>§</sup> University of Illinois.

the structure of Tsukihara et al. (2). Ostermeier et al. (4) argued that the inconsistencies in distance in the two structures from *P. denitrificans* are real and attributed it to a difference in either the crystal packing or the pH of the samples (5.5 vs 8). In recent studies of Tsukihara, Yoshikawa, and co-workers (5) on the reduced protein, the iron–copper distance is found to be 5.2 Å for the ligand-free form and 5.3 Å for the CO-bound form. Also, in the new structural analysis, the Fea<sub>3</sub>–Cu<sub>B</sub> distance in the oxidized protein is 4.9 Å (5).

The crystal structures also reveal that Cu<sub>B</sub> has three histidine ligands, H284, H333, and H334, consistent with the conclusions drawn from the spectroscopic studies (7, 11, 18). (We adopt here the *Rhodobacter sphaeroides* sequence numbering. The corresponding residues in the bovine protein are H240, H290, and H291, respectively, and for the *P. denitrificans* enzyme, they are H276, H325, and H326, respectively.) One of the histidines, H333, is located close to the formyl group of heme a<sub>3</sub> (Figure 1). Another histidine of Cu<sub>B</sub> (H284) is oriented toward a tyrosine residue, Y288 (Y244 in bovine and Y280 in *P. denitrificans*), whose hydroxyl side chain is located within hydrogen-bonding distance of the hydroxy group of the farnesyl side chain of heme a<sub>3</sub>. This tyrosine is very highly conserved among the heme–copper oxidases and is the terminal residue in the K channel, which is postulated to be a proton channel that is involved in the uptake of protons during the initial reduction of the cytochrome a<sub>3</sub>–Cu<sub>B</sub> binuclear center. Thus, the residue is postulated to play a critical functional role during the redox process of delivering protons to the catalytic site during the reduction of the heme–copper center. Very interestingly, it has been shown recently that Y288 is connected by a covalent link formed by a post-translational modification to the adjacent histidine (H284) (4, 5). The functional role of the post-translational modification is not known. However, a structural role for this tyrosine was suggested from mutation studies of this residue (18). Mutation of this residue to phenylalanine in cytochrome b<sub>0</sub> resulted in the loss of Cu<sub>B</sub> (19–21).

To evaluate further the role of Y288, we have made the phenylalanine mutant (Y288F) of the aa<sub>3</sub> oxidase from *R. sphaeroides*. In addition to it not having the hydroxyl group, we postulate that Y288F will not undergo the post-translational modification and will thereby allow for the study of the properties of the binuclear center in the absence of the cross-link. The post-translational linkage may play several functional roles. It may modulate the p*K* of the tyrosine. It may stabilize a radical species that has been postulated to be present during formation of certain intermediates in the catalytic cycle (4, 5, 22). It may stabilize copper in its trivalent oxidation state that has also been postulated to be present during turnover (23). Finally, the cross-linking may provide rigidity and a scaffolding for maintaining the Cu<sub>B</sub> ligands and stabilize the active site geometry. If, in the absence of the cross-link, the binuclear center collapses, it is essential to know what structural changes occur so as to better understand the features that lead to the unique characteristics of this catalytic center in the wild-type enzyme.

In this report, we used optical absorption and resonance Raman spectroscopies to examine the properties of the Y288F mutant enzyme under a variety of conditions.

Resonance Raman spectroscopy is an extremely useful probe for studying heme proteins since specific marker bands in the spectra of oxidases are available that can distinguish the oxidation and spin states of the central iron atom of each of the heme groups (24–26). Furthermore, resonance Raman scattering also provides very useful information concerning the iron–axial ligand modes that have proven to be useful for characterizing heme pocket structure and for following oxygen reduction kinetics (8, 12, 13, 16). On the basis of this work, we propose that one role of the post-translational modification is to allow histidine ligands to coordinate to Cu<sub>B</sub> rather than to the heme iron atom, thereby stabilizing the functionally active site of the enzyme.

## EXPERIMENTAL PROCEDURES

Site-directed mutagenesis was used to form the Y288F mutant of cytochrome *c* oxidase from *R. sphaeroides* (18). The *R. sphaeroides* strain, JS100, has a deletion of the *ctaD* gene which encodes the first subunit of the aa<sub>3</sub>-type cytochrome *c* oxidase. JS100 was transformed with the plasmid that encodes the *ctaD* gene, including the Y288F mutation and an additional six-histidine tag. The cells were grown and harvested as previously reported (27). Ni<sup>2+</sup>–nitrilotriacetic acid agarose affinity chromatography was used to purify the wild type and the Y288F mutant of aa<sub>3</sub>-type cytochrome *c* oxidases, both containing a modified six-histidine tag. Phosphate buffer at pH 8.0 was used instead of Tris for Ni–NTA column chromatography. The samples were concentrated to ~100 μM using a Centricon 100 apparatus (Amicon). PD-10 salt exchange columns (Pharmacia Biotech) were used to remove the Ni<sup>2+</sup> column eluent which was replaced by a buffer of either 10 mM phosphate or Tricine (pH 7.0) and 5% glycerol. The protein samples were frozen in liquid nitrogen for storage. To determine the metal content, an inductively coupled plasma optical emission spectrometer (Perkin-Elmer) was used.

Resonance Raman measurements were taken with enzyme samples (20–30 μM) dissolved in 100 mM phosphate buffer (pH 7.4) containing 3% glycerol and 0.1% lauryl maltoside. The excitation sources for the Raman experiments were the 413.1 nm line of a krypton ion laser (Spectra Physics) and the 441.6 nm line from a He–Cd laser (Liconix). The procedures for taking the Raman measurements have been described in detail elsewhere (28). Briefly, the sample cell was spun at 3000–6000 rpm to minimize local heating. The Raman scattered light was dispersed through a polychromator (Spex, Metuchen, NJ) equipped with a 1200 grooves/mm grating and detected by a liquid nitrogen-cooled CCD camera (Princeton Instruments, Princeton, NJ). A holographic notch filter (Kaiser, Ann Arbor, MI) was used to remove the laser scattering. Typically, several 30 s spectra were recorded and averaged after removal of cosmic ray spikes by a standard software routine (CSMA, Princeton Instruments). The spectral slit width was kept at 5 cm<sup>–1</sup>. Frequency shifts in the Raman spectra were calibrated using indene or acetone–CCl<sub>4</sub> as references.

## RESULTS

The extent of steady-state turnover (rate of ferrocyclochrome *c* reduction) of the “as-isolated” Y288F mutant is negligible. The optical absorption spectrum of the as-isolated

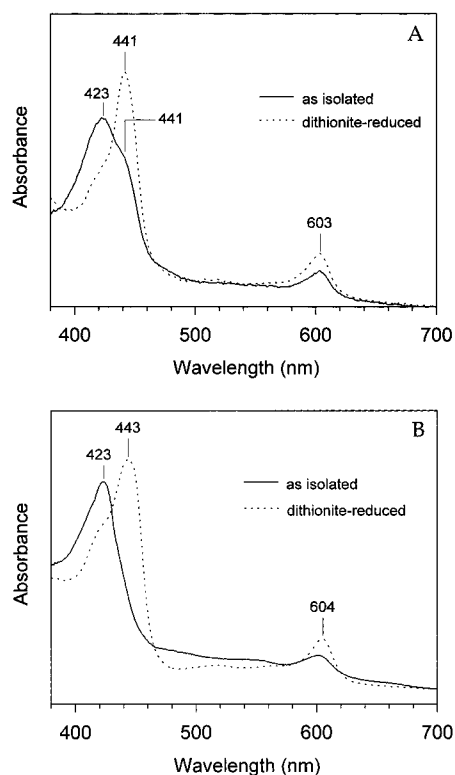


FIGURE 2: Optical absorption spectra of the Y288F mutant (A) and wild type (B) of *R. sphaeroides* in the as-isolated (solid line) and dithionite-reduced (dotted line) states in 100 mM phosphate, 3% glycerol, and 0.1% lauryl maltoside (pH 7.4). The shoulder at 441 nm in the spectrum of the as-isolated Y288F mutant indicates that the hemes are not fully oxidized.

Y288F  $aa_3$  mutant (Figure 2A) of *R. sphaeroides* is different from that of the wild-type enzyme (Figure 2B) but fully consistent with heme *a* prosthetic groups. The presence of heme *a* and the absence of other types of heme were confirmed by pyridine hemochromogen analysis. The wild-type preparation has an absorption maximum at 423 nm in the resting (as-isolated) state, while in the reduced state, the maxima are at 443 and 604 nm. The mutant shows a Soret band at 423 in the resting (as-isolated) state with a very prominent shoulder at 441 nm along with a significant increase in the intensity of the  $\sim 605$  nm band. When the mutant was reduced by ferrocyanide (ascorbate and cytochrome *c*), the bands at 441 and  $\sim 605$  nm increased slightly; however, on addition of dithionite, a completely reduced spectrum was obtained with a slightly different Soret band (at 441 nm) compared to the reduced spectrum of the wild-type enzyme. The metal analysis showed that the Cu content was 0.7 Cu atom less in the Y288F mutant than in the wild type. Complete loss of  $\text{Cu}_B$  was observed in the mutant of the same tyrosine in quinol oxidase (19–21).

The resonance Raman spectra of the Y288F mutant (A) and the wild-type (B) enzymes obtained under the same conditions used for the optical spectra are shown in Figure 3. The resting (as-isolated) wild-type enzyme has a spectrum characteristic of those for other resting oxidases (spectrum a in Figure 3B) (24–26). The electron density-sensitive band, assigned as  $\nu_4$ , is located at 1370  $\text{cm}^{-1}$ , demonstrating that both heme groups are in their fully oxidized state. This is confirmed by the frequencies of the line attributed to the formyl stretching mode from cytochrome *a* at 1643  $\text{cm}^{-1}$  and cytochrome  $a_3$  at 1671  $\text{cm}^{-1}$ . The line at 1570  $\text{cm}^{-1}$

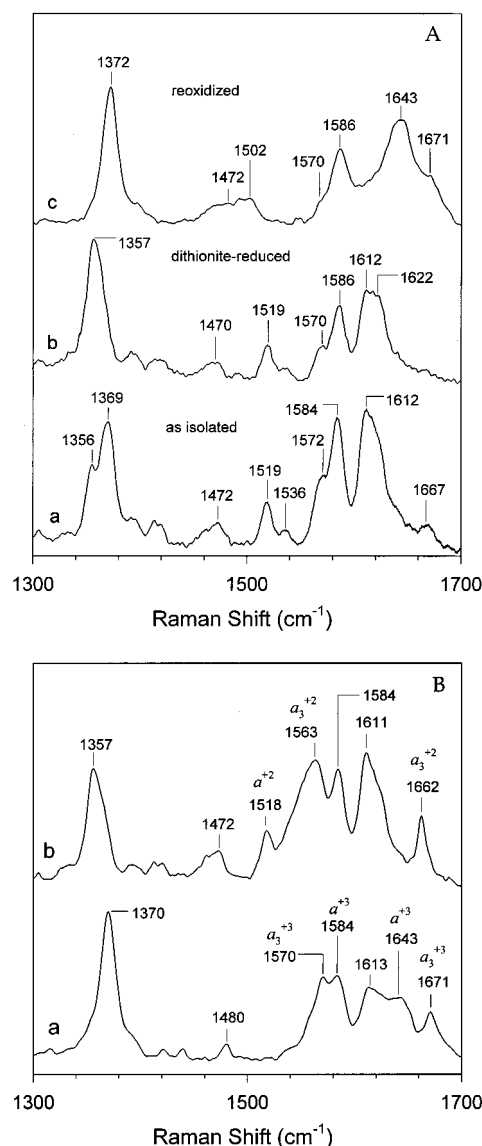


FIGURE 3: Resonance Raman spectra of the Y288F mutant (A) and wild type (B)  $aa_3$  from *R. sphaeroides* in the high-frequency region. Spectra of the Y288F mutant (A) in its as-isolated (a), dithionite-reduced (b), and ferricyanide-oxidized (c) states are shown. For comparison and assignments, spectra of the as-isolated (a) and dithionite-reduced (b) states of the wild-type enzyme (B) are also shown. The excitation frequency was 413.1 nm, and the power delivered at the sample was 6 mW. Some of the marker bands in the wild-type enzyme are identified that are characteristic of different oxidation states of *a* and  $a_3$ . The protein (30  $\mu\text{M}$ ) used for Raman measurements was dissolved in 100 mM phosphate buffer, 3% glycerol, and 0.1% lauryl maltoside (pH 7.4).

originates from the high-spin configuration of ferric cytochrome  $a_3$ , and that at 1584  $\text{cm}^{-1}$  originates from the low-spin configuration of ferric cytochrome *a*. The changes upon reduction, shown in spectrum b of Figure 3B, are also typical of those expected of oxidases, characterized by a shift in  $\nu_4$  from 1370 to 1357  $\text{cm}^{-1}$ , the appearance of the line at 1518  $\text{cm}^{-1}$  from reduced cytochrome *a*, and the shift of the cytochrome *a* and  $a_3$  formyl lines to  $\sim 1611$  and 1662  $\text{cm}^{-1}$ , respectively. In addition, the line at 1563  $\text{cm}^{-1}$  signifies the presence of five-coordinate heme  $a_3$ .

A comparison of the high-frequency resonance Raman spectra of the mutant enzyme (Figure 3A) with that of the wild type (Figure 3B) shows significant differences. The



as-isolated mutant enzyme (spectrum a of Figure 3A) displays a split electron density-sensitive marker line ( $\nu_4$ ) (1356 and 1369  $\text{cm}^{-1}$ ) that indicates that the enzyme has a mixture of oxidized (or possibly oxygenated, but see below) and reduced hemes. Furthermore, the presence of a strong line at 1519  $\text{cm}^{-1}$  and the absence of the line at 1643  $\text{cm}^{-1}$  that was present in the resting state of the wild-type enzyme signify that in the mutant, cytochrome *a* is in its reduced state. Unlike the wild-type enzyme, which has a prominent line at 1570  $\text{cm}^{-1}$  characteristic of the high-spin configuration of cytochrome *a*<sub>3</sub>, the Y288F mutant exhibits only a weak shoulder in this region. Moreover, the strong band at 1584  $\text{cm}^{-1}$  indicates the presence of a low-spin species in Y288F. The observation of the shoulder at 1572  $\text{cm}^{-1}$  may be due to the presence of a small population of a high-spin species. This is consistent with the EPR spectrum (data not shown) which also indicates the presence of a minor high-spin contribution. The formyl line at 1667  $\text{cm}^{-1}$  in Y288F is significantly weaker than that in the wild type. To determine if the as-isolated Y288F mutant enzyme could be converted to a typical resting type of spectrum, the enzyme was oxidized with ferricyanide, and spectrum c in Figure 3A was obtained. This spectrum is characteristic of six-coordinate low-spin hemes with no indication of the high-spin heme that is associated with oxidized cytochrome *a*<sub>3</sub> in the wild-type enzyme. This is indicated by the line at 1570  $\text{cm}^{-1}$  in the wild-type enzyme which is completely absent in the spectrum of the oxidized mutant. Reduction of the reoxidized mutant enzyme with ferrocyanide recovered the as-isolated spectrum (data not shown). Thus, the mutant enzyme is capable of accepting electrons from cytochrome *c*, thereby reducing cytochrome *a*, but no electron transfer from cytochrome *a* to cytochrome *a*<sub>3</sub> occurs.

When the Y288F mutant enzyme is reduced by dithionite, the  $\nu_4$  mode becomes a single line at 1357  $\text{cm}^{-1}$ , indicating reduction of both hemes (spectrum b in Figure 3A). However, there is no line at 1563  $\text{cm}^{-1}$  (other than a weak feature at 1570  $\text{cm}^{-1}$ ), and the formyl line from cytochrome *a*<sub>3</sub> (1662  $\text{cm}^{-1}$  in the reduced *aa*<sub>3</sub> of the wild type) is completely absent. With the exception of the absence of the line from the formyl group of cytochrome *a*<sub>3</sub>, the spectrum of the reduced Y288F mutant enzyme is very similar to that of the fully reduced enzyme when the heme is six-coordinate by a non-electron withdrawing group such as cyanide (25). To test for the possibility of six-coordinate character, we recorded the low-frequency spectrum under conditions in which the iron–histidine stretching mode at 213  $\text{cm}^{-1}$  is prominent for five-coordinate cytochrome *a*<sub>3</sub>. As seen in Figure 4, this mode is present in the wild-type enzyme but is completely absent in the Y288F mutant. It is likely that in the mutant the same sixth ligand is present in the oxidized (as-isolated) and the reduced oxidation states, giving rise to six-coordinate character in both cases.

Since the heme appears to be six-coordinate in Y288F, one might expect that it cannot be oxidized by oxygen. However, we found that upon addition of oxygen to the dithionite-reduced sample we reobtained the spectrum of the as-isolated enzyme. The mechanism of the oxidation of the six-coordinate heme by oxygen is not known, although transient replacement of the sixth ligand by O<sub>2</sub> and its subsequent release from the ferric heme as superoxide is a

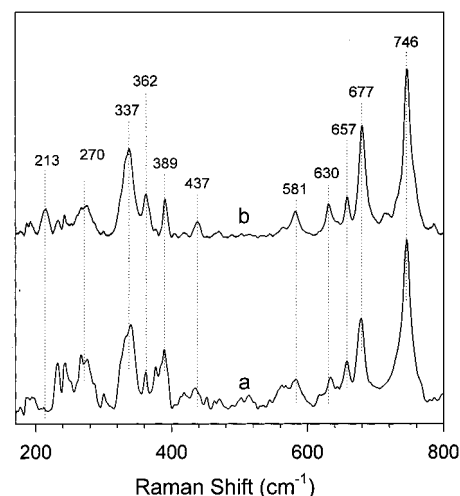


FIGURE 4: Resonance Raman spectra of the Y288F mutant (a) and the wild-type (b) *aa*<sub>3</sub> from *R. sphaeroides* in the low-frequency region in their dithionite-reduced states. The excitation frequency was 441.6 nm, and the power delivered at the sample was 16 mW. The sample conditions are the same as those in the legend of Figure 3.

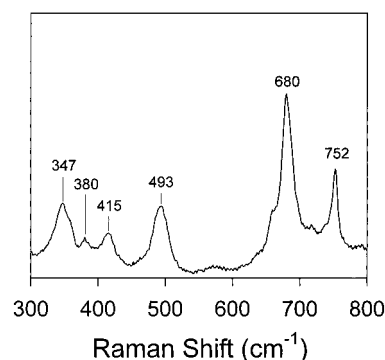


FIGURE 5: Resonance Raman spectra of the CO-bound Y288F mutant of *aa*<sub>3</sub> from *R. sphaeroides* in the low-frequency region. The CO derivative was formed by passing CO gas over the fully reduced (dithionite) protein. The excitation frequency was 413.1 nm, and the power delivered at the sample was ~1 mW. The sample conditions are similar to those in Figure 3.

possibility. However, whereas cytochrome *a*<sub>3</sub> becomes oxidized, cytochrome *a* remains reduced.

The Fe–CO stretching frequency ( $\nu_{\text{Fe-CO}}$ ) in the carbon monoxide derivatives of hemoproteins is known to be sensitive to the electronic and steric nature of the heme pocket. The CO derivative of the wild-type *aa*<sub>3</sub> of *R. sphaeroides* was shown to have two  $\nu_{\text{Fe-CO}}$  modes at 519 and 493  $\text{cm}^{-1}$  at neutral pH corresponding to two conformations of the binuclear site which have been termed the  $\alpha$ - and  $\beta$ -conformations, respectively (27). Recently, we have observed that these two conformations are pH-dependent and hence reflect a polarity change of the binuclear site induced by protons (30, 31). The Y288F mutant shows only one conformer that has a  $\nu_{\text{Fe-CO}}$  at 493  $\text{cm}^{-1}$  at neutral pH (Figure 5). The  $\nu_{\text{Fe-CO}}$  mode remains the same in the pH range of 6.5–9, indicating that the binuclear center lost its ability to participate in proton-induced conformational changes.

## DISCUSSION

The conclusions from the optical and the resonance Raman spectra of the Y288F mutant of the *aa*<sub>3</sub> oxidase from *R.*

*sphaeroides* are quite clear. The as-isolated mutant enzyme is a mixture of oxidized cytochrome  $a_3$  and reduced cytochrome  $a$ ; i.e., it is a mixed-valence species (however, not to be confused with the frequently used mixed-valence terminology that designates an oxidized cytochrome  $a$  center and a reduced cytochrome  $a_3$  center). In the mutant, cytochrome  $a_3$  cannot be reduced by the addition of cytochrome  $c$ , but only by the addition of dithionite. In addition, cytochrome  $a_3$  is largely six-coordinate low-spin in both oxidation states rather than having high-spin configurations as in functional forms of the wild-type enzyme. We postulate that the significant changes observed in the mutant enzyme as compared to the wild type occur because the post-translational modification (Y288–H284 cross-linking) does not take place in the Y288F mutant.

We first consider the structural implications of these observations. The cytochrome  $a_3$  heme is largely six-coordinate in both the oxidized and the reduced states of the Y288F mutant. In the crystal structure of the resting state of wild-type *P. denitrificans aa<sub>3</sub>*, it has been suggested that Cu<sub>B</sub> may have a hydroxide ligand in addition to the three histidine ligands, and a water molecule is attached to the sixth coordination site of the iron atom in cytochrome  $a_3$  (4). This water is not expected to remain bound to the ferrous  $a_3$  heme and, thus, cannot account for the sixth ligand in the reduced form of Y288F. A hydroxide ligand also would not be expected to coordinate to the ferrous heme iron. Since exogenous ligands can be excluded, it is likely that in the Y288F mutant an endogenous ligand is coordinated to the iron atom which would not readily dissociate in either oxidation state. Examination of the heme pocket from the reported crystal structures severely restricts the possible ligands that can coordinate to the heme. In the absence of a complete restructuring of the binuclear center, the only potential heme ligands are the histidines that are normally coordinated to Cu<sub>B</sub>. Three histidines coordinate to the copper, H284, H333, and H334, in the wild-type enzyme. H333 and H334 are on the same helix and are not close to the iron atom of the heme, so it is unlikely that they can coordinate to the heme. H284 is the histidine that forms the covalent post-translational modification with Y288 in the wild-type enzyme. In the absence of the post-translational modification, the histidine may become free to coordinate to the heme. Thus, we assign it as the likely sixth ligand in cytochrome  $a_3$  of the Y288F mutant, although we recognize that one of the other histidines could also serve as the heme ligand depending on the extent of the disruption of the heme pocket. Additional studies are needed to make a definitive determination. Our observation that oxygen can oxidize cytochrome  $a_3$  suggests that the sixth ligand in the mutant is relatively loosely bound and can be readily displaced.

We postulate that in the Y288F mutant, H284 or one of the other histidines coordinates to the heme from the distal side and loses its coordination to Cu<sub>B</sub>. The effect of this is an overall opening of the binuclear center. This relaxation is manifested by movement of Cu<sub>B</sub> away from the iron of cytochrome  $a_3$ , changes in the interactions of the heme group with its environment, and loss of Cu<sub>B</sub> in ~70% of the molecules. The change in the relationship between the iron of cytochrome  $a_3$  and the Cu<sub>B</sub> center is most readily seen by the Fe–C stretching mode of the Fe–CO moiety, which is pH-insensitive in the mutant and is located at 493 cm<sup>–1</sup>.

Specifically, three different forms of the enzyme have been found in both bacterial and mammalian wild-type enzymes and labeled as  $\alpha$ ,  $\beta$ , and  $\delta$ , according to frequencies of the Fe–C–O modes (J. Wang et al., unpublished results). Conversion between these forms is pH-sensitive and has been attributed to changes in the iron–copper distance. The frequency we detect in the Y288F mutant is that which we assign to a  $\delta$  structure in which the copper atom has moved far from the heme such that when CO is bound to the heme it does not interact with the copper; i.e., the pocket is completely open. These results are consistent with the FTIR studies on the Y288 mutant in cytochrome *bo<sub>3</sub>* (21) where a very broad band with multiple features was assigned to the C–O stretching mode of the Fe–CO moiety. The loss of the histidine ligand to the copper in the *aa<sub>3</sub>* enzyme of *R. sphaeroides* causes the disruption of the heme pocket. From the chemical analysis, we conclude that some molecules retain Cu<sub>B</sub> whereas it is lost in others. In both cases, the heme pocket adopts an open structure in which no residues or atoms are as close to the heme binding site as in the wild-type protein.

The absence of Tyr-288 in the heme pocket results in not only the loss of the covalent cross-linking to H284 but also the hydrogen-bonding interaction between the hydroxy group on the tyrosine and the hydroxy group on the farnesyl chain of heme  $a_3$ . That heme  $a_3$  undergoes a change in its conformation in the mutant is shown by the substantial weakening of the formyl line in the resonance Raman spectrum. This change in conformation does not result from movement of the iron into the heme plane in its low-spin form, since the line is always present in the time-resolved resonance Raman spectra of the dioxygen reaction cycle when the enzyme passes through various low- and high-spin forms (D. L. Rousseau, unpublished results). Furthermore, the line is also present in the spectrum of the CO adduct of ferrous cytochrome  $a_3$  (24) and in the spectra of the cyanide adducts of both ferrous and ferric cytochrome  $a_3$  (25). We postulate that the formyl line is resonance-enhanced only when cytochrome  $a_3$  is in its native conformation. In the Y288F mutant, an altered heme  $a_3$  conformation apparently does not permit an extended  $\pi$ -electron conjugation to the formyl group, probably due to a change in the orientation of the latter.

In the resting state of cytochrome *c* oxidase preparations from both bacterial and bovine sources, all the metal centers are in their oxidized forms. This is a consequence of the enzymatic cycle in the presence of oxygen in which following the reduction of oxygen the enzyme returns to the resting oxidized state. However, when isolated, the Y288F mutant is partially reduced, demonstrating that this mutant is unable to undergo a full redox cycle. Both electronic absorption and resonance Raman spectra of the mutant show that the cytochrome  $a$  center is reduced in the as-isolated state as well as in the ferrocycytochrome *c* reduced state, but cytochrome  $a_3$  remains in the oxidized state. It is possible that these observations are a consequence of a blocked electron or proton transfer channel due to the mutation. However, we believe that the most likely explanation that can account for these observations is the possibility that the redox potential of cytochrome  $a_3$  is lowered below that of cytochrome *c*.

Our data clearly show that cytochrome  $a_3$  is six-coordinate in both oxidation states of Y288F. Since histidine is the most reasonable candidate for the sixth ligand, we must consider its effect on the redox potential. Certainly, it could be lowered to be the same as that of cytochrome  $a$  which is also a bis-histidine ligated heme. In addition, the reduction potential is sensitive to a variety of factors, so depending on the environment, the change in the reduction potential could be very large. For example, in myoglobin, when residues near the heme were mutated, changes as large as 200 mV were observed (32). Similarly, in cytochrome  $c$  when the methionine axial ligand is replaced by an imidazole, the reduction potential is lowered by 450 mV (33). In ferric cytochrome P450, a lowering of the redox potential of 150 mV is observed that is associated with the conversion from the high-spin state to the low-spin state (34). A plausible explanation of our data is that with the formation of the six-coordinate low-spin cytochrome  $a_3$ , the redox potential has been lowered below that of cytochrome  $c$ . Thus, in the Y288F mutant, the heme cannot be reduced by ferrocyanide although it can be reduced by dithionite.

When Y288 is mutated to phenylalanine, it is postulated that the cross-linking to H284, a ligand of  $\text{Cu}_B$ , can no longer occur and the structure of the binuclear center becomes severely disrupted. It is likely that the cross-linking holds the heme  $a_3$ - $\text{Cu}_B$  structure in the right configuration for the reduction of dioxygen. Without the cross-linking of Y288 and H284, the heme pocket becomes floppy and one of the histidines normally bound to  $\text{Cu}_B$  coordinates to the heme of cytochrome  $a_3$ , rendering the enzyme inactive. Hence, the post-translational modification of the tyrosine-histidine couple is not accidental, but rather has a well-defined function of holding the binuclear center in a proper configuration to facilitate rapid oxygen binding that leads to a smooth enzymatic cycle.

## REFERENCES

- Iwata, S., Ostermeier, C., Ludwig, B., and Michel, H. (1995) *Nature* 376, 660–669.
- Tsukihara, T., Aoyama, H., Yamashita, E., Tomizaki, T., Yamaguchi, H., Shinzawa-Itoh, K., Nakashima, R., Yaono, R., and Yoshikawa, S. (1995) *Science* 269, 1069–1074.
- Tsukihara, T., Aoyama, H., Yamashita, E., Tomizaki, T., Yamaguchi, H., Shinzawa-Itoh, K., Nakashima, R., Yaono, R., and Yoshikawa, S. (1996) *Science* 272, 1136–1144.
- Ostermeier, C., Harrenga, A., Ermler, U., and Michel, H. (1997) *Proc. Natl. Acad. Sci. U.S.A.* 94, 10547–10553.
- Yoshikawa, S., Shinzawa-Itoh, K., Nakashima, R., Yaono, R., Yamashita, E., Inoue, N., Yao, M., Fei, M. J., Libeu, C. P., Mizushima, T., Yamaguchi, H., Tomizaki, T., and Tsukihara, T. (1998) *Science* 280, 1723–1729.
- Gennis, R. B. (1998) *Science* 280, 1712–1713.
- Babcock, G. T., and Wikstrom, M. (1992) *Nature* 356, 301–309.
- Ferguson-Miller, S., and Babcock, G. T. (1996) *Chem. Rev.* 96, 2889–2907.
- Chan, S. I., and Li, P. M. (1990) *Biochemistry* 29, 1–12.
- Gennis, R. B., and Ferguson-Miller, S. (1996) *Curr. Biol.* 6, 36–38.
- Garcia-Horsman, J. A., Barquera, B., Rumbley, J., Ma, J., and Gennis, R. B. (1994) *J. Bacteriol.* 176, 5587–5600.
- Han, S., Ching, Y. C., and Rousseau, D. L. (1990) *Nature* 348, 89–90.
- Han, S., Ching, Y. C., and Rousseau, D. L. (1990) *Proc. Natl. Acad. Sci. U.S.A.* 87, 8408–8412.
- Woodruff, W. H., Einarsdottir, O., Dyer, R. B., Bagley, K. A., Palmer, G., Atherton, S. J., Goldbeck, R. A., Dawes, T. D., and Kliger, D. S. (1991) *Proc. Natl. Acad. Sci. U.S.A.* 88, 2588–2592.
- Palmer, G. (1993) *J. Bioenerg. Biomembr.* 25, 145–151.
- Kitagawa, T., and Ogura, T. (1997) *Prog. Inorg. Chem.* 45, 431–479.
- Brunori, M., Antonini, G., Malatesta, F., Sarti, P., and Wilson, M. T. (1988) in *Heme Proteins* (Eichhorn, G. L., and Marzilli, L. G., Eds.) Vol. 7, pp 93–153, Elsevier, New York.
- Hosler, J. P., Ferguson-Miller, S., Calhoun, M. W., Thomas, J. W., Hill, J., Lemieux, L., Ma, J., Georgiou, C., Fetter, J., Shapleigh, J., Tecklenburg, M. J., Babcock, G. T., and Gennis, R. B. (1993) *J. Bioenerg. Biomembr.* 25, 121–136.
- Mogi, T., Minagawa, J., Hirano, T., Sato-Watanabe, M., Tsubaki, M., Uno, T., Hori, H., Nakamura, H., Nishimura, Y., and Anraku, Y. (1998) *Biochemistry* 37, 1632–1639.
- Kawasaki, M., Mogi, T., and Anraku, Y. (1997) *J. Biochem.* 122, 422–429.
- Thomas, J. W., Calhoun, M. W., Lemieux, L. J., Puustinen, A., Wikstrom, M., Alben, J. O., and Gennis, R. B. (1994) *Biochemistry* 33, 13013–13021.
- Gennis, R. B. (1998) *Biochim. Biophys. Acta* 1365, 241–248.
- Fabian, M., and Palmer, G. (1995) *Biochemistry* 34, 13802–13810.
- Argade, P. V., Ching, Y. C., and Rousseau, D. L. (1986) *Biophys. J.* 50, 613–620.
- Ching, Y. C., Argade, P. V., and Rousseau, D. L. (1985) *Biochemistry* 24, 4938–4946.
- Babcock, G. T. (1988) in *Biological Applications of Raman Spectroscopy* (Spiro, T. G., Ed.) Vol. 3, pp 293–346, John Wiley & Sons, New York.
- Mitchell, D. M., and Gennis, R. B. (1995) *FEBS Lett.* 368, 148–150.
- Wang, J., Caughey, W. S., and Rousseau, D. L. (1996) in *Methods in Nitric Oxide Research* (Feelisch, M., and Stamler, J. S., Eds.) pp 427–454, John Wiley & Sons, New York.
- Wang, J., Takahashi, S., Hosler, J. P., Mitchell, D. M., Ferguson-Miller, S., Gennis, R. B., and Rousseau, D. L. (1995) *Biochemistry* 34, 9819–9825.
- Das, T. K., Mitchell, D. M., Tomson, F. L., Gennis, R. B., and Rousseau, D. L. (1997) *Biophys. J.* 72, A128.
- Mitchell, D. M., Shapleigh, J. P., Archer, A. M., Alben, J. O., and Gennis, R. B. (1996) *Biochemistry* 35, 9446–9450.
- Varadarajan, R., Zewert, T. E., Gray, H. B., and Boxer, S. G. (1989) *Science* 243, 69–72.
- Liu, G., Shao, W., Zhu, S., and Tang, W. (1995) *J. Inorg. Biochem.* 60, 123–131.
- Sligar, S. G., and Murray, R. I. (1986) in *Cytochrome P-450 Structure, Mechanism, and Biochemistry* (Ortiz de Montellano, P. R., Ed.) pp 429–503, Plenum, New York.

BI981500W